Annals of Nuclear Medicine Vol. 20, No. 9, 583–588, 2006

PET kinetic analysis—compartmental model

Hiroshi WATABE,* Yoko IKOMA,** Yuichi KIMURA,*** Mika NAGANAWA***,**** and Miho SHIDAHARA**

*Department of Investigative Radiology, National Cardiovascular Center Research Institute
**Department of Biophysics, Molecular Imaging Center, National Institute of Radiological Sciences
***Positron Medical Center, Tokyo Metropolitan Institute of Gerontology
****Japan Society for the Promotion of Science

PET enables not only visualization of the distribution of radiotracer, but also has ability to quantify several biomedical functions. Compartmental model is a basic idea to analyze dynamic PET data. This review describes the principle of the compartmental model and categorizes the techniques and approaches for the compartmental model according to various aspects: model design, experimental design, invasiveness, and mathematical solution. We also discussed advanced applications of the compartmental analysis with PET.

Key words: PET, compartmental model, pharmacokinetics

1. Introduction

RECENTLY, positron emission tomography (PET) imaging with ^{18}F labeled fluorodeoxyglucose (FDG) has shown great success in tumor detection and cancer staging. Furthermore, PET has been widely accepted as a tool for "molecular imaging," which is regarded as the main paradigm for twenty-first century biology.[1–3] Among several imaging modalities (such as MRI, SPECT, optical imaging) for molecular imaging, PET imaging has several advantages such as high sensitivity and ability for quantitative measurement. However, in order to exploit PET's potential fully, one must understand some basic principles behind PET. Data measured by PET camera are composed of various signals. In order to isolate the component of the signal of interest, a mathematical framework has been developed by several investigators. "Compartmental model" originated from the field of pharmacokinetics and is a commonly used mathematical model for analyzing PET data. Many methods to analyze PET data have been developed based on the compartmental model including the quantification of blood flow,[4] cerebral metabolic rate for glucose,[5] cerebral oxygen utilization[6] and neuroreceptor ligand binding.[7] In this review, the concept of the compartmental model with PET is introduced and several applications by the compartmental model and PET are discussed.

Received October 2, 2006, revision accepted October 2, 2006.

For reprint contact: Hiroshi Watabe, Ph.D., Department of Investigative Radiology, National Cardiovascular Center Research Institute, 5–7–1 Fujishiro-dai, Suita, Osaka 565–8565, JAPAN.

E-mail: watabe@ri.ncvc.go.jp

2. General concepts for compartmental model to analyze PET data

In a typical PET study, PET data are sequentially obtained after the radioactive tracer is introduced (usually administrated intravenously) over time. By applying proper corrections for attenuation, dead-time of detector, physical decay of radioactivity and scattered photons, PET data represent the tracer concentration (Bq/m*l*) at a certain time. In order to interpret the observed PET data over time, we assume there are physiologically separate pools of tracer substance as "compartments." Figure 1 represents general four compartments model or three tissue compartments model. The first compartment is the arterial blood. From arterial blood, the radioligand passes into the second compartment, known as the free compartment. The third compartment is the region of specific binding which we are usually interested to observe. The fourth compartment is a nonspecific-binding compartment that exchanges with the free compartment. The transport and binding rates of the tracer (K_1 [m*l*$\cdot$ g$^{-1}\cdot$min^{-1}], k_2 [min^{-1}], k_3 [min^{-1}], k_4 [min^{-1}], k_5 [min^{-1}] and k_6 [min^{-1}] in Fig. 1) are assumed to be linearly related

to the concentration differences between two compartments, and the following differential equations are described at time t [min].

$$\frac{dC_b(t)}{dt} = k_3C_f(t) - k_4C_b(t)$$

$$\frac{dC_f(t)}{dt} = K_1C_p(t) + k_6C_n(t) + k_4C_b(t) - (k_2 + k_3 + k_5)C_f(t)$$

$$\frac{dC_n(t)}{dt} = k_5C_f(t) - k_6C_n(t) \tag{1}$$

where $C_p(t)$, $C_f(t)$, $C_b(t)$ and $C_n(t)$ are radioactivity concentrations at time t [min] for each compartment. Data obtained by PET camera ($C_{PET}(t)$) are a summation of these compartments as

$$C_{PET}(t) = C_f(t) + C_b(t) + C_n(t) \tag{2}$$

The parameters can be estimated by fitting the model to measured PET data with arterial radioactivity concentration ($C_p(t)$) as input function. The $C_p(t)$ must be measured separately from PET data acquisition. The frequent manual sampling of the arterial blood or continuous radioactivity monitoring by external radiation detector[8,9] is required (there are several techniques to avoid blood sampling, which will be discussed later).

It is sometimes more useful to employ combinations of the parameters as "macro parameter" to represent the observed data rather than individual parameter. The frequently used macro parameters are distribution volume (K_1/k_2), and binding potential ($\frac{K_1k_3}{k_2k_4}$ or $\frac{k_3}{k_4}$). These estimated parameters or the macro parameters provide several useful pieces of information such as the behavior of target molecule, physiological function, and pharmacokinetics.

There are several assumptions that underlay the compartmental model to interpret PET data. Physiological process and molecular interactions are not influenced by injected radioligand and should be constant during PET measurement. Because PET imaging has sensitivity of 10^{-11}–10^{-12} mol/l, most PET studies fulfill this assumption. We presume that each compartment is homogeneous and the radioligand that passes from one compartment to the other is instantaneously mixed in the compartment.

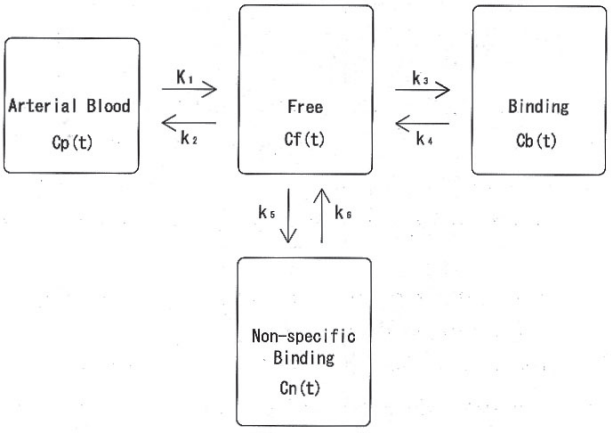

Fig. 1 General three tissue (or four-compartments) compartmental model. This model consists of components of plasma, free ligand in tissue, specific binding and non-specific binding and six rate constants (K_1–k_6).

3. Classification of the compartmental models and analyzes

Many compartmental models and many methods have been proposed to analyze PET data. In this section, we classify the models and methods in different aspects.

3.1 Number of the compartments

The answer for how many compartments must be considered depends on the chemical and biological properties of the radioligand. Moreover, the three tissue compartmental model in Figure 1 has six parameters and the statistical quality of the observed PET data or the statistical properties of the defined model often does not allow to estimate six parameters at once. By reducing the number of the compartments, the number of estimated parameters is reduced and the statistical variability of the parameters is suppressed.

The simplest compartmental model is the model which has only one tissue compartment (Fig. 2). The most popular application of the single-tissue compartment is blood flow measurement by ^{15}O labeled water and PET based on the Fick principle.[4] The single-tissue compartmental model is sometimes enough for many radioligands to describe their kinetics. The neuroreceptor ligand actually behaves under the two or three tissue compartmental model; however, practically one tissue compartmental model is sufficient to describe the kinetics of the ligand in some cases.[10,11]

The two tissue compartmental model (Fig. 3) fits many radioligand tracers well. [^{18}F]FDG is a typical example of the two tissue compartmental model. For many neuroreceptor radioligands, rapid equilibrium between the nonspecific-binding and free compartments can be assumed and the two tissue compartmental model is enough to interpret the kinetics of the ligand.

If the injected radioligand is metabolized and the me-

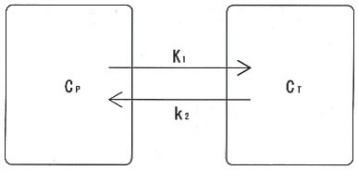

Fig. 2 Single tissue compartmental model. This model has only one compartment in tissue and exchange radiotracer between plasma compartment (C_P) and tissue compartment (C_T) by two rate constants K_1 and k_2.

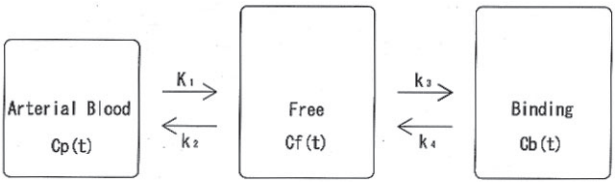

Fig. 3 Two tissue (or three-compartments) compartmental model. This model consists of components of plasma, free ligand (plus non-specific binding) in tissue and specific binding and four rate constants (K_1–k_4).

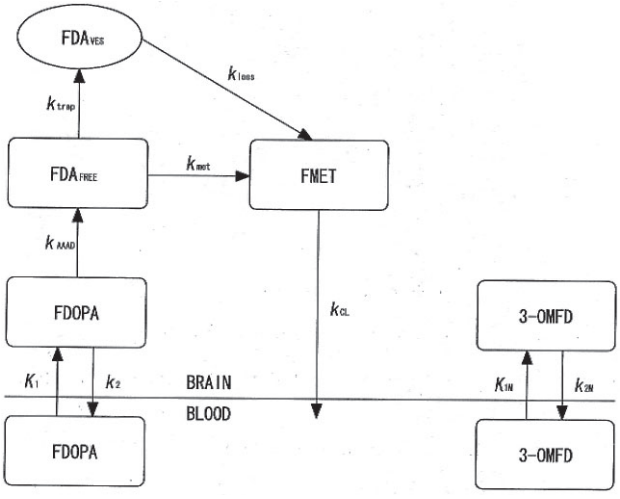

Fig. 4 Compartmental model of FDOPA metabolism.[12] The model consists of FDOPA, fluorodopamine (FDA), FDA metabolites (FMET consist of [^{18}F]6-fluoro-L-3,4-dihydroxyphenylacetic acid, [^{18}F]6-fluorohomovanillic acid) and 3-*O*-methyl-fluorodopa (3-OMFD).

tabolized compounds are detectable by the PET camera, the compartmental model must take into account the kinetics of the metabolites, which results in more compartments and parameters to be estimated. [^{18}F]6-fluoro-L-dopa (FDOPA) is a typical example of these kinds of radioligands (See Fig. 4).[12]

Alternatively, there are several approaches which do not require assumption of the number of compartments. Instead, they estimate the macro parameters such as the distribution volume based on common properties among the compartmental models. Graphical approaches by Patlak et al.[13] and Logan et al.[14] estimate the macro parameter by graphically fitting a straight line to the transformed experimental data. Spectral analysis[15,16] assumes that the observed PET data can be described by sets of exponentials as impulse response function and employs non-negative least squares fitting to estimate exponential basis functions. The spectral analysis also supplies information on the number of compartments. The basis pursuit denosing[17] extends the concept of the spectral analysis and permits negative coefficient for the basis functions, facilitating adaptation for the reference tissue model (see below for explanation of the reference tissue model).

3.2 Bolus or infusion administration of the radiotracer

In many cases, the radiotracer is administrated as a bolus, and dynamic changes of PET data are observed and analyzed. As shown in Eq. 1, the compartmental model mathematically includes differential equations. If equilibrium condition is achieved, i.e. the change rate of the concentration against time in the compartment is zero, the left side of Eq. 1 becomes zero, which simplifies mathematical formulations for the compartmental analysis. Continuously supplying radiotracer may produce equilibrium condition. Well established technique using this strategy is measurements of cerebral blood flow and oxygen consumption by continuous inhalations of ^{15}O–CO, ^{15}O–CO_2 and ^{15}O–O_2 gases.[18] Another example of usage of the equilibrium condition is bolus plus constant infusion paradigm for neuroreceptor study.[19] This experimental paradigm starts with bolus injection of the radiotracer followed by continuously infused administration of the radiotracer to achieve constant concentrations in the tissue and blood. The distribution volume and binding potential can be easily obtained by calculating ratios between the radioactivity concentrations in the tissues and blood. The rate of the infusion may vary between subjects, and optimal scheduling of the experiments must be sought for success of the bolus plus infusion paradigm.[20]

3.3 Compartmental analysis with the arterial input function or without the arterial input function

As described above, the arterial radioactivity curve as the input curve is essential for the compartmental analysis with PET. However, arterial sampling is invasive and technically demanding. If the heart chamber is inside the field-of-view of PET camera, the arterial input function can be directly derived from PET images.[21,22] Or the input function is estimated by extracting components of blood from PET images by means of image-processing.[23,24]

Alternatively, several techniques based on compartmental analysis have been developed. A common strategy for these techniques is omitting the arterial input function by assuming that all pixels of the interest in the PET data share the same arterial input function.[25–28] Many radioligands for neuroreceptor use the reference tissue model (Fig. 5) of Lammertsma et al.[27] or its extensions.[29] Although these techniques have several advantages over the method with the arterial input function, especially non-invasiveness, these techniques generally have more assumptions and need caution for use. For example, the existence of the specific binding in the reference region result in an underestimation of specfic binding in the target region.[30]

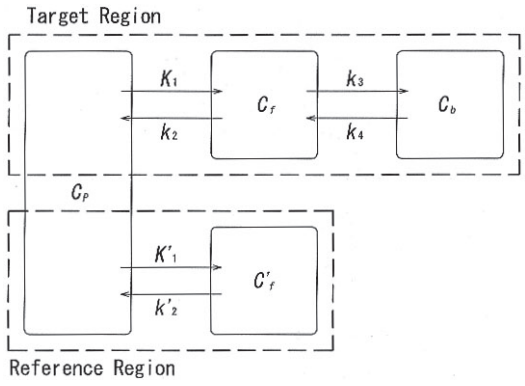

Fig. 5 Reference tissue model.[27] The target region and the reference region have the same plasma input function. It uses the C'_f, time activity curve of the reference region as an indirect input function.

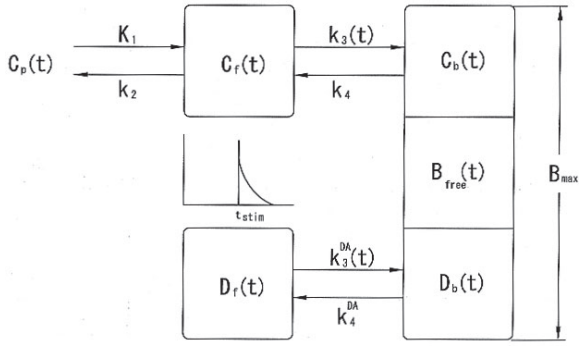

Fig. 6 Extended receptor model which accounts for dopamine competition.[37] Amphetamine is introduced at time t_{stim}, and endogenous dopamine is released. The parameter k_3 is varied according to free receptor B_{free}.

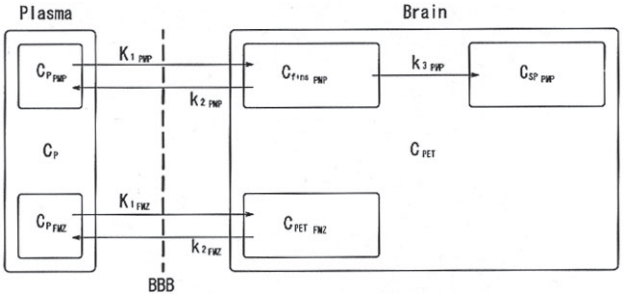

Fig. 7 Combined compartmental model for dual injections of PMP and DTBZ or FMZ.[38]

3.4 Non-linear or linear fitting

In order to estimate parameters from Eqs. 1 and 2, non-linear least squares fitting procedure is required. Generally, the non-linear fitting procedure is computationally expensive. Several graphical approaches[13,14,31,32] are available to make non-linear problems into linear ones, which results in quick estimation of parameters. One must select the proper graphical approach for a particular radiotracer. For instance, Patlak plot[13] must be applied for irreversible tracer and Logan plot[14] for reversible tracer. The statistical bias may be introduced due to noise in PET data, and the improper selection of the graphical approach leads to wrong parameter estimation.[32,33] Basis function approach[34,35] is another major method for linearization. In this approach, non-linear terms of solution for the compartmental model are discretely precalculated within available ranges of the kinetic parameters, which results in a linear system to solve. Although the method is computationally more demanding than the graphical approaches, the method allows determination of the individual kinetic parameters of the model.

4. Advanced applications using the compartmental analysis

As mentioned above, the compartmental model assumes that kinetic parameters are constant during the experiment. By intentionally violating this assumption, however, PET can detect and quantify transient changes in neurotransmitter concentrations.[36] Endres et al.[37] extended the compartmental model to consider endogenous dopamine release (Fig. 6) and showed that PET data were well fitted to the model.

Recently, there has been growing interest in detecting multiple functions simultaneously within the same subject by multiple injections of radiotracer. Koeppe et al.[38] developed a combined compartmental model (Fig. 7) and studied dual injections of [^{11}C]flumazenil (FMZ), *N*-[^{11}C]methylpiperidinyl propionate (PMP) and [^{11}C]dihydrotetrabenazine (DTBZ). Kudomi et al.[39] developed a model which compensates for the background radioactivity from a previously injected radiotracer and computes CBF and $CMRO_2$ from a single PET acquisition with a sequential administration of [^{15}O]O_2 and [^{15}O]H_2O.

As molecular imaging, many trials are currently underway to image reporter gene expression *in vivo* using PET. The compartmental model can play a role to quantify kinetics of the reporter protein. Green et al.[40] showed that the kinetics of ^{18}F-FHBG can be represented by a two-tissue compartmental model, and k_3 is an index of activity of the reporter protein. However, there are still several issues remaining for quantification of therapeutic gene expression[41] and further investigations are required. One particular problem is that the time scale observed by PET may differ from that for gene expression.

5. Conclusion

The compartmental model is a basic concept to quantitatively evaluate PET data. Many techniques based on the compartmental model have been developed as described in this review and one must select the most appropriate technique to analyze one's own PET data. In future, the

compartmental model will play an important role in molecular imaging.

REFERENCES

1. Luker G, Piwnica-Worms D. Molecular imaging *in vivo* with PET and SPECT. *Acad Radiol November* 2001; 8: 4–14.
2. Dobrucki L, Sinusas A. Molecular imaging. A new approach to nuclear cardiology. *Q J Nucl Med Mol Imaging* 2005; 49 (1): 106–115.
3. Weissleder R. Molecular imaging in cancer. *Science* 2006; 312 (5777): 1168–1171.
4. Kety S. The theory and applications of the exchange of inert gas at the lungs and tissues. *Pharmacol Rev* 1951; 3: 3–41.
5. Reivich M, Kuhl D, Wolf A, Greenberg J, Phelps M, Ido T, et al. The [^{18}F]fluorodeoxyglucose method for the measurement of local cerebral glucose utilization in man. *Circ Res* 1979; 44 (1): 127–137.
6. Mintun M, Raichle M, Martin W, Herscovitch P. Brain oxygen utilization measured with O-15 radiotracers and positron emission tomography. *J Nucl Med* 1984; 25 (2): 177–187.
7. Mintun M, Raichle M, Kilbourn M, Wooten G, Welch M. A quantitative model for the *in vivo* assessment of drug binding sites with positron emission tomography. *Ann Neurol* 1984; 15 (3): 217–227.
8. Eriksson L, Holte S, Bohm C, Kesselberg M, Hovander B. Automated blood sampling systems for positron emission tomography. *IEEE Nucl Sci* 1988; 35 (1): 703–707.
9. Kudomi N, Choi E, Yamamoto S, Watabe H, Kim K, Shidahara M, et al. Development of a GSO detector assembly for a continuous blood sampling system. *IEEE Trans Nucl Sci* 2003; 50 (1): 70–73.
10. Koeppe R, Holthoff V, Frey K, Kilbourn M, Kuhl D. Compartmental analysis of [^{11}C]flumazenil kinetics for the estimation of ligand transport rate and receptor distribution using positron emission tomography. *J Cereb Blood Flow Metab* 1991; 11 (5): 735–744.
11. Watabe H, Channing M, Der M, Adams H, Jagoda E, Herscovitch P, et al. Kinetic analysis of the 5-HT2A ligand [^{11}C]MDL 100,907. *J Cereb Blood Flow Metab* 2000; 20 (6): 899–909.
12. Endres C, Endres C, DeJesus O, DeJesus O, Uno H, Uno H, et al. Time profile of cerebral [^{18}F]6-fluoro-L-DOPA metabolites in nonhuman primate: implications for the kinetics of therapeutic L-DOPA. *Front Biosci* 2004; 9: 505–512.
13. Patlak C, Blasberg R. Graphical evaluation of blood-to-brain transfer constants from multiple-time uptake data. Generalizations. *J Cereb Blood Flow Metab* 1985; 5 (4): 584–590.
14. Logan J, Fowler J, Volkow N, Wolf A, Dewey S, Schlyer D, et al. Graphical analysis of reversible radioligand binding from time-activity measurements applied to *N*-[^{11}C]methyl-(–)-cocaine PET studies in human subjects. *J Cereb Blood Flow Metab* 1990; 10 (5): 740–747.
15. Cunningham V, Jones T. Spectral analysis of dynamic PET studies. *J Cereb Blood Flow Metab* 1993; 13 (1): 15–23.
16. Murase K. Spectral analysis: principle and clinical applications. *Ann Nucl Med* 2003; 17 (6): 427–434.
17. Gunn R, Gunn S, Turkheimer F, Aston J, Cunningham V. Positron emission tomography compartmental models: a basis pursuit strategy for kinetic modeling. *J Cereb Blood Flow Metab* 2002; 22 (12): 1425–1439.
18. Lammertsma A, Jones T, Frackowiak R, Lenzi G. A theoretical study of the steady-state model for measuring regional cerebral blood flow and oxygen utilisation using oxygen-15. *J Comput Assist Tomogr* 1981; 5 (4): 544–550.
19. Carson R, Channing M, Blasberg R, Dunn B, Cohen R, Rice K, et al. Comparison of bolus and infusion methods for receptor quantitation: application to [^{18}F]cyclofoxy and positron emission tomography. *J Cereb Blood Flow Metab* 1993; 13 (1): 24–42.
20. Watabe H, Endres C, Breier A, Schmall B, Eckelman W, Carson R. Measurement of dopamine release with continuous infusion of [^{11}C]raclopride: optimization and signal-to-noise considerations. *J Nucl Med* 2000; 41 (3): 522–530.
21. Iida H, Kanno I, Takahashi A, Miura S, Murakami M, Takahashi K, et al. Measurement of absolute myocardial blood flow with $H_2{}^{15}O$ and dynamic positron-emission tomography. Strategy for quantification in relation to the partial-volume effect. *Circulation* 1988; 78 (1): 104–115.
22. Choi Y, Huang S, Hawkins R, Kim J, Kim B, Hoh C, et al. Quantification of myocardial blood flow using ^{13}N-ammonia and PET: comparison of tracer models. *J Nucl Med* 1999; 40 (6): 1045–1055.
23. Watabe H, Channing M, Riddell C, Jousse F, Libutti S, Carrasquillo J, et al. Noninvasive estimation of the aorta input function for measurement of tumor blood flow with [^{15}O]water. *IEEE Trans Med Imaging* 2001; 20 (3): 164–174.
24. Naganawa M, Kimura Y, Ishii K, Oda K, Ishiwata K, Matani A. Extraction of a plasma time-activity curve from dynamic brain PET images based on independent component analysis. *IEEE Trans Biomed Eng* 2005; 52 (2): 201–210.
25. Watabe H, Itoh M, Cunningham V, Lammertsma A, Bloomfield P, Mejia M, et al. Noninvasive quantification of rCBF using positron emission tomography. *J Cereb Blood Flow Metab* 1996; 16 (2): 311–319.
26. Bella ED, Clackdoyle R, Gullberg G. Blind estimation of compartmental model parameters. *Phys Med Biol* 1999; 44 (3): 765–780.
27. Lammertsma A, Bench C, Hume S, Osman S, Gunn K, Brooks D, et al. Comparison of methods for analysis of clinical [^{11}C]raclopride studies. *J Cereb Blood Flow Metab* 1996; 16 (1): 42–52.
28. Lammertsma A, Hume S. Simplified reference tissue model for PET receptor studies. *Neuroimage* 1996; 4 (3 Pt 1): 153–158.
29. Endres C, Bencherif B, Hilton J, Madar I, Frost J. Quantification of brain muopioid receptors with [^{11}C]carfentanil: reference-tissue methods. *Nucl Med Biol* 2003; 30 (2): 177–186.
30. Kropholler MA, Boellaard R, Schuitemaker A, Folkersma H, Berckel BNMV, Lammertsma AA. Evaluation of reference tissue models for the analysis of [^{11}C](R)-PK11195 studies. *J Cereb Blood Flow Metab* 2006.
31. Yokoi T, Iida H, Itoh H, Kanno I. A new graphic plot analysis for cerebral blood flow and partition coefficient with iodine-123-iodoamphetamine and dynamic SPECT

validation studies using oxygen-15-water and PET. *J Nucl Med* 1993; 34 (3): 498–505.
32. Ichise M, Toyama H, Innis R, Carson R. Strategies to improve neuroreceptor parameter estimation by linear regression analysis. *J Cereb Blood Flow Metab* 2002; 22 (10): 1271–1281.
33. Slifstein M, Laruelle M. Effects of statistical noise on graphic analysis of PET neuroreceptor studies. *J Nucl Med* 2000; 41 (12): 2083–2088.
34. Gunn R, Lammertsma A, Hume S, Cunningham V. Parametric imaging of ligand-receptor binding in PET using a simplified reference region model. *Neuroimage* 1997; 6 (4): 279–287.
35. Watabe H, Watabe H, Jino H, Jino H, Kawachi N, Kawachi N, et al. Parametric imaging of myocardial blood flow with ^{15}O-water and PET using the basis function method. *J Nucl Med* 2005; 46 (7): 1219–1224.
36. Breier A, Su T, Saunders R, Carson R, Kolachana B, Bartolomeis de A, et al. Schizophrenia is associated with elevated amphetamine-induced synaptic dopamine concentrations: evidence from a novel positron emission tomography method. *Proc Natl Acad Sci USA* 1997; 94 (6): 2569–2574.
37. Endres C, Kolachana B, Saunders R, Su T, Weinberger D, Breier A, et al. Kinetic modeling of [^{11}C]raclopride: combined PET-microdialysis studies. *J Cereb Blood Flow Metab* 1997; 17 (9): 932–942.
38. Koeppe R, Raffel D, Snyder S, Ficaro E, Kilbourn M, Kuhl D. Dual-[^{11}C]tracer single-acquisition positron emission tomography studies. *J Cereb Blood Flow Metab* 2001; 21 (12): 1480–1492.
39. Kudomi N, Hayashi T, Teramoto N, Watabe H, Kawachi N, Ohta Y, et al. Rapid quantitative measurement of $CMRO_2$ and CBF by dual administration of ^{15}O-labeled oxygen and water during a single PET scan—a validation study and error analysis in anesthetized monkeys. *J Cereb Blood Flow Metab* 2005; 25: 1209–1224.
40. Green L, Nguyen K, Berenji B, Iyer M, Bauer E, Barrio J, et al. A tracer kinetic model for ^{18}F-FHBG for quantitating herpes simplex virus type 1 thymidine kinase reporter gene expression in living animals using PET. *J Nucl Med* 2004; 45 (9): 1560–1570.
41. Richard J, Zhou Z, Chen D, Mintun M, Piwnica-Worms D, Factor P, et al. Quantitation of pulmonary transgene expression with PET imaging. *J Nucl Med* 2004; 45 (4): 644–654.